Control of Colloid Surface Chemistry through Matrix Confinement: Facile Preparation of Stable Antibody Functionalized Silver Nanoparticles

Lynell R. Skewis and Björn M. Reinhard*

Department of Chemistry and The Photonics Center, Boston University, Boston, Massachusetts 02215

ABSTRACT Here we describe a simple yet efficient gel-matrix-assisted preparation method that improves synthetic control over the interface between inorganic nanomaterials and biopolymers and yields stable biofunctionalized silver nanoparticles. Covalent functionalization of the noble metal surface is aided by the confinement of polyethylene glycol acetic acid functionalized silver nanoparticles in thin slabs of a 1% agarose gel. The gel-confined nanoparticles can be transferred between reaction and washing media simply by immersing the gel slab in the solution of interest. The agarose matrix retains nanoparticles but is swiftly penetrated by the antibodies of interest. The antibodies are covalently anchored to the nanoparticles using conventional cross-linking strategies, and the resulting antibody functionalized nanoparticles are recovered from the gel through electroelution. We demonstrate the efficacy of this nanoparticle functionalization approach by labeling specific receptors on cellular surfaces with functionalized silver nanoparticles that are stable under physiological conditions.

KEYWORDS: immunolabeling • nanoplasmonics • bioconjugation • nanoscale imaging • smart nanoparticles • particle tracking

INTRODUCTION

Noble metal nanoparticles are enabling materials for a wide range of applications in diverse fields such as nanophotonics, electronics, diagnostics, and therapeutics. Many of these applications, especially in the biomedical field, depend on the ability to functionalize the surface of these materials with biological molecules to convey functionality, selectivity, and stability. Applications of noble metal nanoparticles (colloids) as active components in diagnostics (1−3), biophysics (4−6), and nanotechnology (7−9) require particles with well-defined surfaces, low nonspecific binding background, and excellent stability in the required buffer medium. Gold (Au) and silver (Ag) nanoparticles are particularly useful labels as they have large optical cross-sections, superb photostabilities (10, 11), and are amenable to multimodal imaging in the optical microscope, electron microscope, and X-ray microscope. Controlled application of these nanomaterials under physiological conditions is, however, often complicated by their limited stability in the elevated salt concentrations and complex chemical environment of the solution.

Currently Au nanoparticles are predominantly chosen over Ag nanoparticles for biological imaging applications because they are easier to prepare and functionalize, and they remain stable in higher salt concentrations. Ag nanoparticles, given their larger scattering cross sections and narrower plasmon resonances (12), could enable smaller probes with higher sensitivities for the detection of refractive index or interparticle separation changes. Additionally, in aqueous solution, Ag nanoparticles of 20−40 nm diameters scatter strongly in the blue, a region of relatively low cellular scattering background (see below). Despite these advantages, the preparation of antibody functionalized Ag of a size that produces enough signal for high temporal resolution optical imaging (20−40 nm) and remain stable in the physiological buffers has proven difficult. Under such conditions, screening of the stabilizing charge of the nanoparticles results in aggregation, and Ag nanoparticles can undergo oxidative corrosion (13). Some progress has been made in synthesizing stable Ag−DNA conjugates (14). However, to exploit the advantageous optical properties of Ag nanoparticles for challenging applications such as selective immunolabeling with low background, improved preparative strategies for particle stabilization and specific antibody functionalization are required.

The most straightforward approach to biofunctionalize noble metal nanoparticles is by noncovalent attachment of antibodies to the metal surface through electrostatic attraction. This method yields probes with many active groups; however, the shell of antibodies increases the effective size of the probe significantly, while providing insufficient stability of Ag particles under high salt conditions.

Another method that offers superior stabilization and a well-defined surface involves the formation of a self-assembled monolayer of short thiolated alkyl polyethylene glycol acetic acids ($HSC_{11}H_{22}(OC_2H_4)_6OCH_2COOH$), in the following simply referred to as PEGs, around the particles. The surface group of these ligands can be chosen for desired

* To whom correspondence should be addressed. E-mail: bmr@bu.edu.
Received for review August 6, 2009 and accepted December 7, 2009

DOI: 10.1021/am900822f

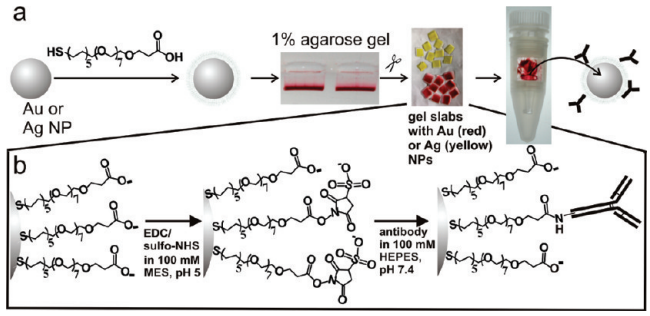

FIGURE 1. Preparation of antibody functionalized 40 nm Au and Ag nanoparticles (NPs). (a) Particles were incubated with a short bifunctional PEG overnight, these stabilized particles were then run into a 1% agarose gel in 100 mM phosphate buffer, pH 7.4. Particle containing slabs were cut and exchanged between activation buffer, cross-linking reagents, and antibody containing coupling buffer. The antibody cross-linked particles were then electroeluted and stored in 0.5% Tris-Borate-EDTA buffer. (b) Details of cross-linking chemistry.

surface charge or cross-linking capabilities. It has been shown that small (2−15 nm) Ag and Au probes with this type of protection (though with −OH or NH_2 replacing −COOH as the surface group) remain stable in 1 M NaCl (13, 15). We have found that this type of ligand also provides excellent protection to 40 nm Ag particles, which are suitable as high-contrast probes for single-molecule imaging.

A common scheme for the biofunctionalization of particles is to apply carboxylic acid as the surface group for cross-linking to primary amines of the desired protein (e.g., antibody or lectin) by 1-ethyl-3-[3-dimethylaminopropyl]-carbodiimide hydrochloride (EDC) and *N*-hydroxysulfocuccinimide (sulfo-NHS). This reaction is pH controlled and requires cleaning and buffer exchange after the formation of the activated NHS-ester (see Figure 1). Because the NHS-ester hydrolyzes in the coupling buffer at pH 7.4, rapid and efficient cleaning and buffer exchange for the "activated" colloid is necessary to optimize yield. We found that centrifugation—the obvious method of cleaning colloids—can induce irreversible aggregation of activated 40 nm Ag-NHS-ester conjugates. Column chromatography is an alternative method for cleaning and buffer exchange; however, this method is not compatible with the quick buffer exchanges desirable to maximize the cross-linking efficiency by minimizing hydrolysis of the NHS-ester intermediate. We describe here a bioconjugation strategy that eliminates aggregation of particles during intermediate cross-linking steps by confining the particles in thin slices of 1% agarose gel. Simply immersing the particle containing slabs in the desired solutions allows for convenient and efficient transfer of the particles between different reaction and washing solutions and thus offers an alternative when conventional functionalization strategies involving centrifugation or column chromatography purifications cannot be applied.

EXPERIMENTAL SECTION

Ag Nanoparticle Functionalization. In the following, we outline our strategy for efficient antibody functionalization of Ag nanoparticles, however, similar conditions also provide for convenient biofunctionalization of Au particles. We incubated 40 nm commercial Ag particles concentrated from 7×10^{10} particles in 1 mL to 50 μL with 5 μL of a 10 mM PEG solution, $HSC_{11}H_{22}(OC_2H_4)_6OCH_2COOH$ in water, for 12 h. These pegylated particles were then run into a 1% agarose gel in a 100 mM, pH 7.4 phosphate running buffer. The pegylated silver particles migrate in a single band, separate from excess PEG ligand. The Ag40 nm-PEG bands were cut from the gel and immersed in 100 mM 2-(*N*-morpholino)ethanesulfonic acid (MES) buffer, pH 5, for 15 min. The gel slabs were then transferred into the cross-linker solution: 2 mM EDC and 5 mM sulfo-NHS in 100 mM MES pH 5. After allowing the activation reaction to proceed for 1 h, the slabs were removed from excess cross-linking solution and rinsed once with coupling buffer, 100 mM 4-(2-hydroxyethyl)-1-piperazineethanesulfonic acid (HEPES) buffer, pH 7.4. The slabs were subsequently immersed in a solution of desired antibody at a concentration of 1 μg/mL in the same coupling buffer. A typical cross-linking reaction of 7×10^{10} Ag nanoparticles (~5 gel slabs) consumed ~2 μg of antibody. The coupling reaction was carried out for 12 h at 4 °C. After the coupling was complete, the antibody functionalized Ag particles were recovered from the gel slabs through electroelution in 0.5 mM Tris/Borate/EDTA (TBE) buffer. The amines of the TBE buffer also served to quench the cross-linking reaction. Subsequently, the nanoparticles were washed and eventually concentrated through centrifugation. Excess antibodies that might have electroeluted from the gel together with the nanopartices were removed in the supernatant.

Confocal Imaging of Antibody Diffusion into 1% Agarose Gel Slabs. Slabs of ~1 mm thickness of 1% agarose gel were placed in a glass-bottomed dish and imaged with an Olympus FV1000 scanning confocal microscope. The gel slab was immersed in a 1 μg/mL solution of Texas-red labeled secondary antibodies in coupling buffer, and the fluorescence was monitored across a 130 μm × 130 μm section approximately 600 nm below the top surface as function of time. Texas-red was excited at 543 μm and the fluorescence emission was detected at 615 nm. Images of the fluorescence intensity were recorded at 5 min intervals for 3 h 45 min. The fluorescence intensity in the gel as function of position and time was extracted from these images using a home written Matlab program.

In vitro Binding Experiments. The interior surfaces of rectangular glass capillary tube flow chambers were functionalized by incubation for 15 min with a 1 mg/mL solution of bovine serum albumin-biotin (BSA-biotin) in 10 mM Tris, 50 mM NaCl, pH 7. This surface provided a binding target for Ag particles functionalized via the above method with antibiotin antibody and controls consisting of Ag particles exposed to cross-linker but no antibody, Ag particles exposed to antibiotin antibody but no cross-linker, and particles exposed to cross-linker and an anti-EGFR antibody that should not bind to the biotinylated surface and thus served as control.

Cell Culture and Membrane Preparation. A431 cells, a human epithelial carcinoma cell line, were cultured in Dulbecco's modified eagle's medium (DMEM) supplemented with L-glutamine, penicillin, and streptomycin in an incubator at 37 °C, 5% CO_2, and 95% relative humidity. Cells to be labeled and imaged were grown on glass coverslips to approximately 30% confluency. For measuring the spectra of Ag labels on the cellular membrane, A431 cells were grown on coverslips then just prior to labeling and imaging the cells were mechanically lysed by sonication in water for approximately 30s.

Dark-Field Microscopy and Spectroscopy. All in vitro binding and live cell scattering images were collected on an Olympus IX71 inverted microscope equipped with a cage incubator for live cell imaging. The cells, in a homemade flow chamber, were imaged under darkfield illumination using unpolarized white light from a 100 W Tungsten or 150 W Xenon lamp. The light scattered in the specimen plane was collected with a 10× objective and imaged with an Andor iXon^{EM+} 897 electron

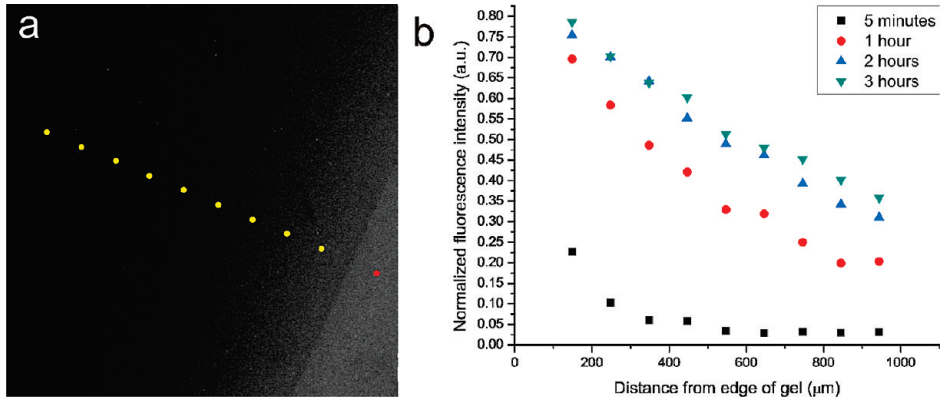

FIGURE 2. Time-resolved diffusion of fluorescently labeled antibodies into 1% agarose gel slab. A 1 mm thick slab of 1% agarose gel was immersed in a 1 μg/mL solution of Texas red-labeled secondary antibody. The fluorescence intensity was monitored for one section (600 μm below the gel surface) with a scanning confocal microscope. (a) Home-written Matlab code was used to extract the fluorescence intensity at various distances into the gel slab (yellow dots) and in the solution (red dot), repeated for several time points. (b) Fluorescence intensity as function of distance from the gel edge was plotted as a function of time.

multiplying charge-coupled device (EMCCD). Color images were recorded with an eyepiece mounted digital camera. Spectra of nanoparticles bound to membranes were obtained on an upright Olympus BX51WI microscope coupled to a 300 mm focal length Andor Shamrock spectrometer using a 60× oil immersion objective and an Andor DU401-BR-DD detector.

RESULTS AND DISCUSSION

Gel-Matrix-Assisted Antibody Functionalization of Ag Nanoparticles. We embedded 40 nm Ag particles in 1 mm thick slabs of agarose gel to improve the efficiency of EDC/sulfoNHS cross-linking of the particles to antibodies by facilitating rapid buffer exchange. The details of this procedure are shown in Figure 1. This method takes advantage of the selective permeability of the gel for antibodies and cross-linking reagent. Due to their larger size, the Ag particles are mostly confined to the pores of the gel, whereas the smaller antibodies can efficiently enter the gel through passive diffusion to react with the activated particles. To confirm that the antibodies enter the gel quickly enough for effective cross-linking, we monitored the penetration of fluorescently labeled antibodies into a gel slab as a function of time (see Figure 2a).

In Figure 2b, we show a plot of the fluorescence intensity (normalized to the intensity of the solution of fluorescently labeled antibodies) at the marked positions in the gel section (illustrated in Figure 2a) as a function of distance from the edge of the gel for four time points. These intensities were measured at a depth of 600 μm into the gel slab. The plot shows that after 5 min, fluorescence was detectable approximately 250 μm into the slab, indicating the presence of antibodies. After an hour, the antibodies had penetrated at least 1 mm (the farthest distance from the slab monitored) into the gel. Subsequently, the fluorescence intensity at all distances increased as the concentration of antibodies in the gel further increased. The half-life of NHS-esters in this pH range is ~4 h (according to the product sheet from Pierce Products). The confocal study shows that the time required for antibodies to diffuse into thin gel slabs is sufficiently low to ensure an efficient cross-linking to the activated particles. Encouraged by this finding, we prepared different antibody functionalized particles using the gel confinement approach and quantified their stability and binding efficiency.

Stability of Antibody-Functionalized Ag Nanoparticles. We investigated the stability of these antibody functionalized particles by monitoring the bulk UV−vis absorbance (Abs) over time in common live cell imaging buffers. Figure 3a shows a time series of absorption for anti-EGFR functionalized 40 nm Ag particles in live cell imaging buffer (Hanks Balanced Salt Solution (HBSS) with Mg^{2+} and Ca^{2+} and 15 mM HEPES pH 7.4, approximately 150 mM NaCl). The peak wavelength of the particles remained centered at 420 nm throughout the observation time of 60 min. The ratio of Abs at 420 and 450 nm remains constant for most of the observation time (see Figure 2b). Only after 50 min does the $Abs_{420\ nm}/Abs_{450\ nm}$ ratio show a slight decrease indicative of a weak spectral red-shift due to low levels of agglomeration. The stability of the PEG-protected Ag particles functionalized using the gel confinement strategy is contrasted by the rapid agglomeration observed for Ag particles to which antibodies were noncovalently attached to the surface. The higher stability of the silver nanoparticles obtained through the gel confinement strategy offers these particles a clear advantage for applications requiring monomeric particles with well-defined optical responses, as is the case for single-particle tracking or plasmon coupling microscopy.

Ideally, the functionalized nanoparticles would not have to be prepared fresh prior to every application, but could be stored for some time after preparation. To ensure sustained activity of the antibodies, storage of the nanoparticle-antibody conjugates at +4° or lower is mandatory. We verified the stability of the antibody functionalized particles when stored at +4°, by monitoring the plasmon resonance of a dilute solution of antibody functionalized nanoparticles in storage buffer of 100 mM HEPES pH 7.4 over a period of 10 days. The absence of any systematic shift in the plasmon resonance of the nanoparticle solution in Figure 3c shows that the nanoparticles show no substantial agglomeration over the monitored time span. Since it is usually not recommended to store antibodies for longer than ~2 weeks at +4

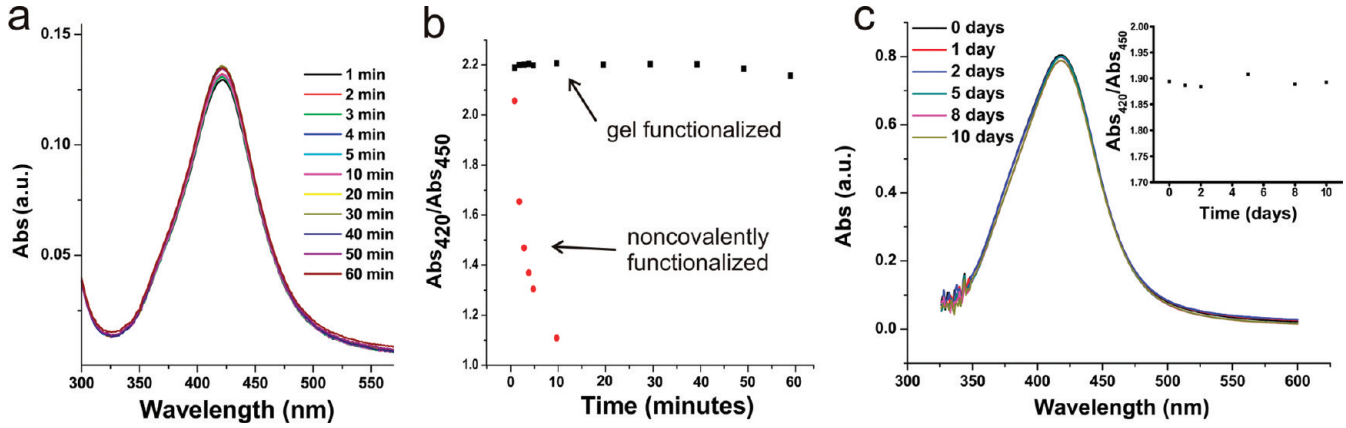

FIGURE 3. Stability of antibody functionalized 40 nm Ag particles in imaging and storage buffers. (a) UV−vis absorbance (Abs) of anti-EGFR functionalized 40 nm Ag particles in imaging buffer. (b) The ratio of Abs at 420 and 450 nm over time for: gel assisted anti-EGFR functionalized 40 nm Ag particles (black), and Ag40 nm particles with noncovalently attached anti-EGFR in imaging buffer (red). (c) Abs of anti-EGFR functionalized 40 nm particles in storage buffer over 10 days. The ratio of Abs at 420 and 450 nm are included in the inset.

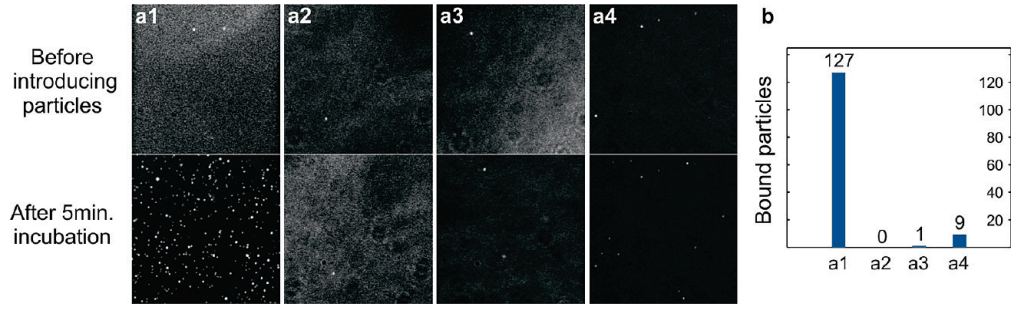

FIGURE 4. In vitro binding experiment of gel-matrix-assisted functionalized particles in a BSA-biotin coated rectangular glass capillary. Dark-field images of coated capillaries exposed to (a1) antibiotin functionalized particles, (a2) cross-linker activated particles with no antibody, (a3) particles exposed to antibiotin but without cross-linker, and (a4) anti-EGFR functionalized particles. (b) Histogram of bound particles as detected by home written Matlab code (see ref 20).

due to on-setting degradation and loss in activity, we did not extend our investigations to longer times. Figure 3c confirms that the functionalized silver nanoparticles can be stored at least for several days in the refrigerator without the risk of inducing nanoparticle agglomeration. This finding is important from an application point of view, because it reduces the frequency with which the particles need to be prepared.

In vitro Binding Experiments Confirm the Specificity of Functionalized Ag Particles. The specificity of stabilized antibody functionalized particles for their targets was confirmed through in vitro binding experiments (see Figure 4). In these experiments, functionalized nanoparticles were flushed into rectangular glass capillary tubes prepared with a biotin surface. Using the gel-matrix-assisted preparation approach, we prepared the following controls: Ag nanoparticles reacted with cross-linker but no antibodies, antibiotin but no cross-linker, and cross-linker with a random antibody (anti-EGFR). Only particles exposed to both cross-linker and antibiotin antibody bound to the biotin surface. None of the controls showed appreciable binding to the surface. This experiment was repeated three times with only slightly varying binding efficiencies. This result confirms that the antibodies were attached covalently to the nanoparticle surface and still bind specifically to their target after conjugation to the nanoparticle.

Binding of anti-EGFR-Functionalized Ag Particles to Live Cells. To further confirm the specificity of these particles and their suitability for live cell studies, we exposed live A431 (human epithelial carcinoma) cells, which overexpress EGFR, to anti-EGFR-Ag40 nm conjugates and an antibiotin conjugate control. The living cells were incubated with the nanoparticle solution (~2×10^{10} particles/mL) in imaging buffer at 37 °C in a home-built flow chamber mounted on an inverted dark-field microscope with cage incubator. After an incubation time of 5 min, excess nanoparticles were flushed out of the chamber and the cells were imaged using dark-field microscopy. As illustrated in Figure 5a, in the case of the anti-EGFR functionalized particles, even after this short incubation time we observed clusters of A431 cells with a high density of nanoparticles bound to the cell surface. The stained cells are easily detectable by "eye" through microscopy given their vividly blue color. The antibiotin-functionalized particles showed significantly lower binding levels to the cell surfaces under identical conditions (Figure 5b), confirming that most of the binding in Figure 5a is selective, and the anti-EGFR functionalized nanoparticles bind specifically to the targeted receptors on the cell surface.

The image shown in Figure 5a was taken in a conventional dark-field microscope at 10× magnification. At this magnification, individual cells are clearly distinguishable. Specifically functionalized nanoparticles in combination with darkfield microscopy are thus compatible with single cell identification. The latter underlines the potential value of this

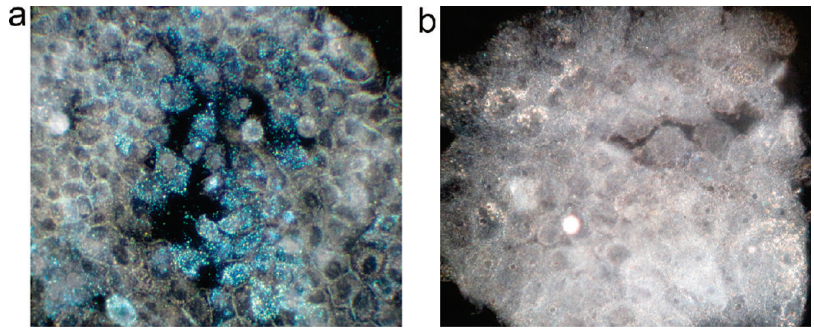

FIGURE 5. Darkfield microscopy (Xenon whitelight illumination) image at 10× magnification of (a) anti-EGFR bound to the surface of living A431 cells and (b) live A431 cells exposed to antibiotin functionalized particles where no binding is observed.

technology, for instance, for single-cell cancer diagnostics, provided the nanoparticles are functionalized with an antibody against a cancer specific biomarker.

Spectroscopy of anti-EGFR-Ag Labels on A431 Membranes. For many applications of nanoparticle labels, for instance in single-particle tracking (16, 17) or plasmon coupling microscopy (6), it is important to validate that the imaged probes are indeed monomeric. Unlike fluorescent probes, for which the number of dyes in a specific subdiffraction limit volume can be quantified by counting bleaching events, noble metal nanoparticles do not bleach. However, the resonance wavelength of a noble metal nanoparticle contains information about the possible aggregation state (2, 11, 12). This relationship facilitates direct experimental confirmation that the anti-EGFR-Ag40 nm labels (prepared by gel matrix assisted cross-linking) bound to the cell surface are monomeric. To optimize signal-to-noise for the spectral calibration of these probes, we elected to measure the spectra of particles targeted to A431 cells that were mechanically lysed by sonication.

Cells attached to glass slides were lysed in live cell imaging buffer, the remaining membranes attached to the slides were labeled with anti-EGFR-Ag40 nm conjugates in 100 mM HEPES, pH 7.4. As shown in Figure 6a, the Ag probes are clearly visible by eye through darkfield microscopy. Figure 6b shows a representative scattering spectrum of an Ag particle and nearby membrane scattering. The plasmon resonance is clearly visible as the strong peak centered at 448 nm. Significant background from the membrane is also apparent but is well-shifted from the plasmon and could be reduced with a band-pass filter. This observation provides further evidence that 40 nm Ag particles are more suitable labels for cell surface components in dark-field microscopy than 40 nm Au particles, as they offer a higher contrast.

To confirm that the observed scattering sources were indeed individual particles, we compared the spectra of particles bound to the membranes with those of individual particles immobilized on a glass surface recorded under identical buffer conditions. The particles on the glass surface were confirmed to be monomers by scanning electron microscopy. The peak wavelength distributions for ~50 random individual emitters recorded on the cell surface and on glass are shown in panels c and d in Figure 6, respectively. These distributions overlay, giving strong evidence

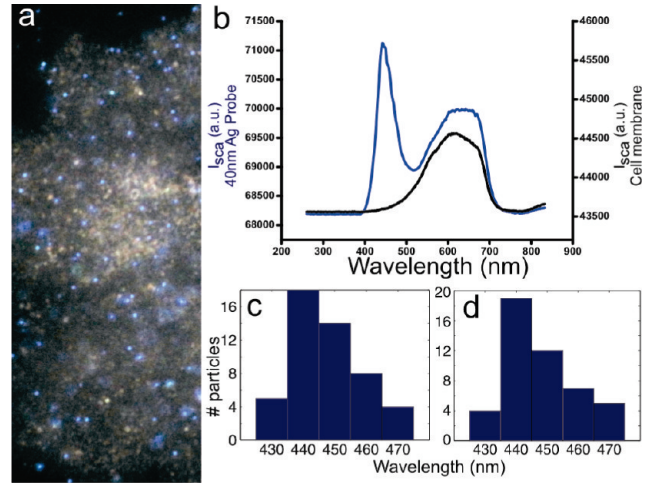

FIGURE 6. Spectral analysis of anti-EGFR functionalized 40 nm Ag labels on A431 membranes. (a) Individual probes are clearly visible in darkfield microscopy. (b) The scattering spectrum (Tungsten whitelight excitation, unprocessed) of a single Ag particle plotted along with the scattering spectra of nearby area of the cell membrane. Distributions of the plasmon resonance wavelength of 50 individual anti-EGFR particles on (c) glass and (d) A431 membrane.

that the membrane labels are monomeric. The lysed cells were more "sticky" than living cells and allowed some nonspecific binding. This non-specific binding of the anti-EGFR nanoparticles did, however, not impede the analysis of their aggregation state.

The role of the silver nanoparticles as immunolabels is only one important application of the generated nanoparticles. Another potential application area is that of local surface plasmon resonance (LSPR) biosensing (18, 19). LSPR is highly dependent on the local environment and the resonance wavelength shift when analytes bind selectively to specifically functionalized nanoparticles. Because of their high polarizability and sharp plasmon resonances Ag nanoparticles enable the detection of even small shifts in the local refractive index and are thus ideal materials for LSPR biosensing. For the detection of a specific analyte in a complex biological sample, stable and specifically functionalized nanoparticles with low nonspecific binding background are required. The matrix confinement surface functionalization approach can provide these materials and will thus contribute to make Ag-nanoparticle-based sensing and imaging more robust.

CONCLUSION

In summary, we have developed a simple, but efficient method to prepare stable, antibody functionalized Ag (and Au) nanoparticle labels for optical microscopy and plasmonic sensing that improves upon existing techniques. We have shown that a gel-matrix-assisted bioconjugation approach yields antibody functionalized probes that are stable under physiological conditions and bind selectively to their cellular targets. The overall duration of the nanoparticle functionalization approach is relatively long (~30 h) but this is mostly due to extended incubation periods. The actual processing steps are, however, short and simple and provide functionalized nanoparticles which can be stored at +4° without risking agglomeration. Because of the scale of the approach, the proposed technology is currently primarily suitable for research applications in advanced biosensing and biophotonics. Because of their large optical cross-section and high polarizability, stable biofunctionalized Ag nanoparticles have the potential to improve existing capabilities in these fields. In addition, mechanistic studies of cell surface processes using single-particle tracking or plasmon coupling require well-defined, stable particles with large optical scattering cross-sections, and the particles provided by the method developed here are ideal for these challenging fundamental studies.

Acknowledgment. We acknowledge financial support from the National Institutes of Health (NIH) through Grants 1R01CA138509-01 and 5R21EB008822-02 (B.M.R.) and a Ruth L. Kirschstein National Research Service Award from the NIH (L.R.S.).

REFERENCES AND NOTES

(1) Anker, J. N.; Hall, W. P.; Lyandres, O.; Shah, N. C.; Zhao, J.; Van Duyne, R. P. *Nat. Mater.* **2008**, *7* (6), 442–453.
(2) Elghanian, R.; Storhoff, J. J.; Mucic, R. C.; Letsinger, R. L.; Mirkin, C. A. *Science* **1997**, *277* (5329), 1078–1081.
(3) Lal, S.; Link, S.; Halas, N. *Nat. Photonics* **2007**, *1* (11), 641–648.
(4) Rong, G. X.; Wang, H. Y.; Skewis, L. R.; Reinhard, B. M. *Nano Lett.* **2008**, *8* (10), 3386–3393.
(5) Skewis, L. R.; Reinhard, B. M. *Nano Lett.* **2008**, *8* (1), 214–220.
(6) Reinhard, B. M.; Sheikholeslami, S.; Mastroianni, A.; Alivisatos, A. P.; Liphardt, J. *Proc. Natl. Acad. Sci. U.S.A.* **2007**, *104* (8), 2667–2672.
(7) Maier, S. A.; Brongersma, M. L.; Kik, P. G.; Meltzer, S.; Requicha, A. A. G.; Atwater, H. A. *Adv. Mater.* **2001**, *13* (19), 1501.
(8) Maier, S. A.; Kik, P. G.; Atwater, H. A.; Meltzer, S.; Harel, E.; Koel, B. E.; Requicha, A. A. G. *Nat. Mater.* **2003**, *2* (4), 229–232.
(9) Ozbay, E. *Science* **2006**, *311* (5758), 189–193.
(10) Kelly, K. L.; Coronado, E.; Zhao, L. L.; Schatz, G. C. *J. Phys. Chem. B* **2003**, *107* (3), 668–677.
(11) Yguerabide, J.; Yguerabide, E. E. *J. Cell. Biochem.* **2001**, 71–81.
(12) Yguerabide, J.; Yguerabide, E. E. *Anal. Biochem.* **1998**, *262* (2), 137–156.
(13) Doty, R. C.; Tshikhudo, T. R.; Brust, M.; Fernig, D. G. *Chem. Mater.* **2005**, *17* (18), 4630–4635.
(14) Lee, J. S.; Lytton-Jean, A. K. R.; Hurst, S. J.; Mirkin, C. A. *Nano Lett.* **2007**, *7* (7), 2112–2115.
(15) Kanaras, A. G.; Kamounah, F. S.; Schaumburg, K.; Kiely, C. J.; Brust, M. *Chem. Commun.* **2002**, (20), 2294–2295.
(16) Orr, G.; Hu, D. H.; Ozcelik, S.; Opresko, L. K.; Wiley, H. S.; Colson, S. D. *Biophys. J.* **2005**, *89* (2), 1362–1373.
(17) Umemura, Y. M.; Vrljic, M.; Nishimura, S. Y.; Fujiwara, T. K.; Suzuki, K. G. N.; Kusumi, A. *Biophys. J.* **2008**, *95* (1), 435–450.
(18) Haes, A. J.; Van Duyne, R. P. *J. Am. Chem. Soc.* **2002**, *124*, 10596–10604.
(19) Zhao, J.; Zhang, X. Y.; Yonzon, C. R.; Haes, A. J.; Van Duyne, R. P. *Nanomedicine* **2006**, *1*, 219–228.
(20) The home-written Matlab code referred to in Figure 4 was based on tracking code in developed by Daniel Blair and Eric Dufrensne and is available at http://physics.georgetown.edu/matlab/index.html.

AM900822F